Desalination and Water Treatment
www.deswater.com
doi: 10.1080/19443994.2014.934728

56 (2015) 146–160
September

Taylor & Francis
Taylor & Francis Group

Biosorption potential assessment of modified pistachio shell waste for methylene blue: thermodynamics and kinetics study

Moonis Ali Khan[a,*], Zeid Abdullah Al Othman[a], Mahendra Kumar[b], Mohammad Shamsul Ola[c], Masoom Raza Siddique[a]

[a]*Chemistry Department, College of Science, King Saud University, Riyadh 11451, Saudi Arabia, Tel. +00966564505403; emails: mokhan@ksu.edu.sa, moonisalikhan@gmail.com (M.A. Khan), Tel. +0096614674198; email: zaothman@ksu.edu.sa (Z.A. Al Othman); email: siddiqui124@gmail.com (M.R. Siddique)*
[b]*School of Biotechnology, Dublin City University, Dublin 9, Ireland, Tel. +00353 1 7005281; email: mahendracsmcri@gmail.com*
[c]*Department of Biochemistry, College of Science, King Saud University, Riyadh 11451, Saudi Arabia, Tel. +00966558013579; email: shamsulola@gmail.com*

Received 4 December 2013; Accepted 4 June 2014

ABSTRACT

Batch scale studies were conducted to investigate biosorption potential of sodium hydroxide treated pistachio shell (PS) biomass for methylene blue (MB). Fourier transform infrared spectroscopy analysis confirmed interaction between acidic oxygen surface groups and MB nitrogen atoms. Scanning electron microscopy, wide angle X-ray diffraction (WXRD) technique, energy dispersive X-ray spectroscopy and N_2 adsorption/desorption isotherm studies were carried out to evaluate surface morphology, surface area and pore size of biomass. Optimum MB biosorption (92.12%) was observed at pH 5.63. A drastic decrease in biosorption from 21.6 to 2.75 mg/g was observed with increase in ionic salt (NaCl) concentration from 0.05 to 0.25 M. Contact time study showed increase in biosorption capacity from 5.75 to 23.07 mg/g with MB concentration (25–100 mg/L). Equilibration time ranged between 60 and 240 min. Biosorption was endothermic and physical process obeying pseudo second order kinetics model. Isotherm studies revealed applicability of Sips model. The MB recovery was 99.8% with 0.15 M oxalic acid (OA) within 15 min. Regeneration study confirmed almost constant recovery rate for four consecutive cycles.

Keywords: Pistachio shell; Alkaline treatment; Physisorption; Desorption; Regeneration

1. Introduction

The effluents discharge from textile, leather tannery, paper and pulp, cosmetic and pharmaceutical industries are generally characterized by high alkalinity, biological oxygen demand (BOD), chemical oxygen demand (COD), total dissolved solids (TDS) adding undesirable color to water bodies [1] depleting dissolved oxygen content and interfere photosynthesis of aquatic plants. More than 100,000 dyes are available commercially and annually more than 7×10^5 metric tons dyes are produced globally [2]. Methylene blue (MB), a cationic dye commonly used for dying cotton, wool and silk [3]. Ingestion of MB may cause nausea, vomiting, profuse sweating and mental confusion. In addition, inhalation of MB creates difficulty in breathing [4]. Concerning the hazardous effects, it is

*Corresponding author.

essential to treat effluents containing MB before being discharged into the water bodies.

Several conventional techniques such photodegradation, chemical coagulation, ion-exchange, chemical oxidation, biodegradation and ozonation have been reported for the removal of dyes from waste effluents. However, these techniques scuffle with several disadvantages such as inefficiency at lower concentration, high energy and chemical reagents requirement, generation of toxic sludge or other wastes as by-product that need careful treatment and disposal, high capital and operational costs, etc. [5]. Due to the aforementioned demerits it is urgent to come up with a process which is economically feasible and ecologically safe. Adsorption is an emerging and attractive method, which involves the sorption of dissolved substances. Moreover, the primary advantages of this method are the reusability of adsorbent, simplicity in design, ease of operation, low operation cost and efficient for the removal of synthetic dyes from wastewater effluents and aqueous solution [6,7].

Various synthetic adsorbents such as magnetic rectorite/iron oxide nanocomposites and halloysite nanotubes [8,9] and biomass (biosorbents) such as succinylated sugarcane bagasse, *Lemna minor*, rice hull ash, acron shell, lignocellulosic material, and bamboo based activated carbon have been utilized for the biosorption of MB from aqueous solution [2, 10–14].

Pistacia vera L. (Pistachio) plant belongs to Anacardiaceae family which is mainly cultivated in the Middle East, Mediterranean countries and the United States. According to Food and Agricultural Organization's (FAO's) statistical analysis, 30 million metrics tons pistachio shell (PS) waste is generated annually by pistachio nut processing industries [15]. Pistachio shell can be used for kindling, mulch for shrubs and plants that requires acid soils, used at the bottom of plant pot to help drainage and in jewellery. Pistachio shell has already been utilized for the removal of Hg(II) [16], Pb(II) [17,18], Zn(II) [19], phenol [20] from aqueous solution. Researchers have also prepared activated carbon from PS as a precursor material by various physico-chemical treatment processes for the removal of dyes and VOCs [15,21–23]. In this study, PS was modified with NaOH (MPS). The biosorption potential of MPS for the removal of MB from aqueous phase was tested. Various experimental parameters such as effect of contact time, initial MB concentration, temperature, ionic salt (NaCl) solution and biomass dosage were comprehensively studied. The economic feasibility of biosorbent was tested by desorption and regeneration studies.

2. Materials and methods

2.1. Chemicals and reagents

Methylene blue (MB), hydrogen peroxide (H_2O_2), hydrochloric acid (HCl) and NaOH were purchased from Sigma-Aldrich, Germany. Nitric acid (HNO_3), sulphuric acid (H_2SO_4), acetic acid (CH_3COOH), formic acid (HCOOH), oxalic acid ($H_2C_2O_4$) and citric acid ($C_6H_8O_7$) were purchased from Winlab Laboratory Chemicals, UK and Merck, Germany. The chemicals and reagents used in this study were of analytical reagent grade or as specified. The stock solution of MB (1,000 mg/L) was prepared by dissolving 1,000 mg of MB in 1 L deionized (DI) water. The standard flask containing MB solution was wrapped with aluminium foil and kept in dark to avoid the photo-degradation of MB solution.

2.2. Preparation of biosorbent

Pistachio shells were collected from the local dry foods supplier. Pistachio shells were washed with DI water to remove dust and dirt. Pistachio shells were dried in oven at 60°C for 24 h. The dried PS were grounded with grinder and sieved to 0.2–0.4 mm particle size. Biomass (PS, 1.0 g) was treated with 100 mL hydrogen peroxide (30% w/w) and the resulting mixture was kept in a water bath shaker at 50°C for 60 min with constant stirring at 100 rpm to oxidize the organic content. Afterwards, the biomass was washed several times with DI water to remove the traces of hydrogen peroxide. The oxidized biomass was again treated with 0.10 M NaOH in a water bath shaker at 25°C for 24 h with constant stirring at 100 rpm. Lower environmental load in its life cycle, less corrosive ability and economic feasibility [24] are the major merits of using NaOH as a modifying agent. The NaOH treated biomass was washed several times with DI water to achieve neutral pH. Resultant biomass was dried in oven at 65°C for 24 h to get constant weight and the modified pistachio shell (MPS) biomass was kept in sealed plastic bags and stored in a desiccator to the avoid moisture contamination. Similar treatment procedure was adopted for the modification of PS biomass with 0.10 M HCl and 0.10 M $HClO_4$.

2.3. Characterization of biomass

The FTIR spectra of biosorbent were recorded using a Varian 3100 spectrometer, USA. The spectra were recorded in the range from 600 to 4,000 cm^{-1} with an average of 32 scans at a ±4.0 cm^{-1} resolution. Scanning electron microscope coupled with energy disperse

X-ray (SEM-EDX) (Quanta 400 FEG, Czech Republic) at an electron acceleration voltage of 15 kV was used to evaluate biomass surface morphology and elemental content. The wide angle X-ray diffraction (WXRD) pattern of biosorbent was recorded using a Philips Xpert WXRD with nickel-filtered CuKα radiation (1.54056). The biomass surface area was analyzed at 303 K using a static volumetric system ASAP 2020 surface area and pore size analyzer (Micromeritics Inc., USA). The specific surface area of biosorbent was determined from N_2 adsorption isotherm at 77.35 K.

2.4. Experimental methodology

Batch biosorption studies were carried out in 100 mL stopper cork conical flasks. The 25 mL MB solutions of known concentrations were equilibrated with 0.25 g of MPS for 24 h in a temperature controlled water bath shaker with constant stirring at 120 rpm. At equilibration, the samples were filtered using Whatman filter No. 40 and the concentration of MB in supernatant solution was measured by UV–vis Spectrophotometer (Thermo Scientific Evolution 600, UK). The percentage of biosorption and biosorption capacity (q_e) were calculated using the Eqs. (1) and (2), respectively.

$$\%\text{Biosorption} = \frac{(C_0 - C_e)}{C_0} \times 100 \quad (1)$$

$$q_e(mg/g) = (C_0 - C_e) \times \frac{V}{m} \quad (2)$$

where, C_0 and C_e are the initial and equilibrium concentrations of MB (mg/L), V is the volume of solution (L) and m is the mass of MPS (g).

The pH study was carried out at 25 mg/L initial concentration of MB solution. The initial pH of MB solution was adjusted from 2.32 to 10.98 by adding 0.10 M HCl and 0.10 M NaOH solutions. The contact time study was performed by varying the initial concentration of MB solution from 25 to 100 mg/L. The isotherm study was conducted through varying the initial concentration of MB solution from 25 to 200 mg/L and reaction temperature from 298 to 333 K. Dosage study was carried out by varying the amount of MPS from 0.2 to 1.0 g at 100 mg/L initial concentration of MB. The effect of NaCl solution of various concentrations (0.05–0.25 M) on MB biosorption was also tested. Desorption and regeneration studies were carried out by batch mode. The 0.25 g biosorbent was initially saturated with 25 mL MB solution (C_0, 50 mg/L). The equilibration reaction continued for 24 h in a water bath shaker at 120 rpm at 303 K temperature. The saturated biomass was then washed several times with DI water to remove unadsorbed MB traces form biomass surface. Different acids (hydrochloride, HA; nitric acid, NA; sulphuric acid, SA; acetic acid, AA; formic acid, FA; oxalic acid, OA; citric acid, CA) of 0.10 M concentration, alcohols (ethanol, EeOH; methanol, MeOH) and acetone (Ac) were used to elute the adsorbed MB from MPS biomass. After the selection of the best eluent, experiments were conducted at various eluent concentrations for optimum MB elution. For regeneration study, 0.10 g biosorbent was initially equilibrated with 25 mL MB solution (C_o − 100 mg/L) for 24 h in a water bath shaker at 120 rpm at 303 K temperature. Afterwards, saturated biosorbent was washed several times with DI water to remove unadsorbed MB traces, and then treated with 0.15 M OA for the elution of MB. The same procedure was repeated for four consecutive cycles.

3. Results and discussion

The biosorption of MB onto unmodified PS (UPS) was 57%, while optimum MB biosorption (92%) was achieved on MPS. Biosorption on HCl and $HClO_4$ treated PS was 70.7 and 65.1%. Thus, NaOH treated PS (MPS) biomass was selected for further MB biosorption studies.

3.1. Characterization of biomass

The presence of oxygen and nitrogen atoms is mainly responsible for acidic and basic functionalities of the biosorbent. The increase in acidic oxygen surface groups (carbonyl and hydroxyl) is expected to enhance the uptake capacity of the biosorbents. The FTIR studies revealed functional groups present on the surface of PS biosorbent before and after NaOH treatment (Fig. 1(a)). The broad absorption bands at 3,336 cm^{-1} and 2,897 cm^{-1} were attributed to O–H stretching vibration and aliphatic $-CH_2$ groups present on UPS biomass [25]. The major constituents of Pistachio shell biomass are hemicellulose, cellulose and lignin [26]. These constituents were confirmed from the obtained peaks in 1,750–1,500 cm^{-1}, which are attributed to the stretching vibrations of keto -C=O groups (1,732 cm^{-1}) and C=C stretching vibrations of aromatic rings (1,597 and 1,494 cm^{-1}) in lignin. The peaks in 1,500–1,314 cm^{-1} were observed due to bending vibrations of O–H and aliphatic deformation vibration of $-CH_3$ and $-CH_2$ groups present in cellulose and lignin. The absorption bands in 1,300–1,000 cm^{-1} were assigned to stretching vibration of C–O in

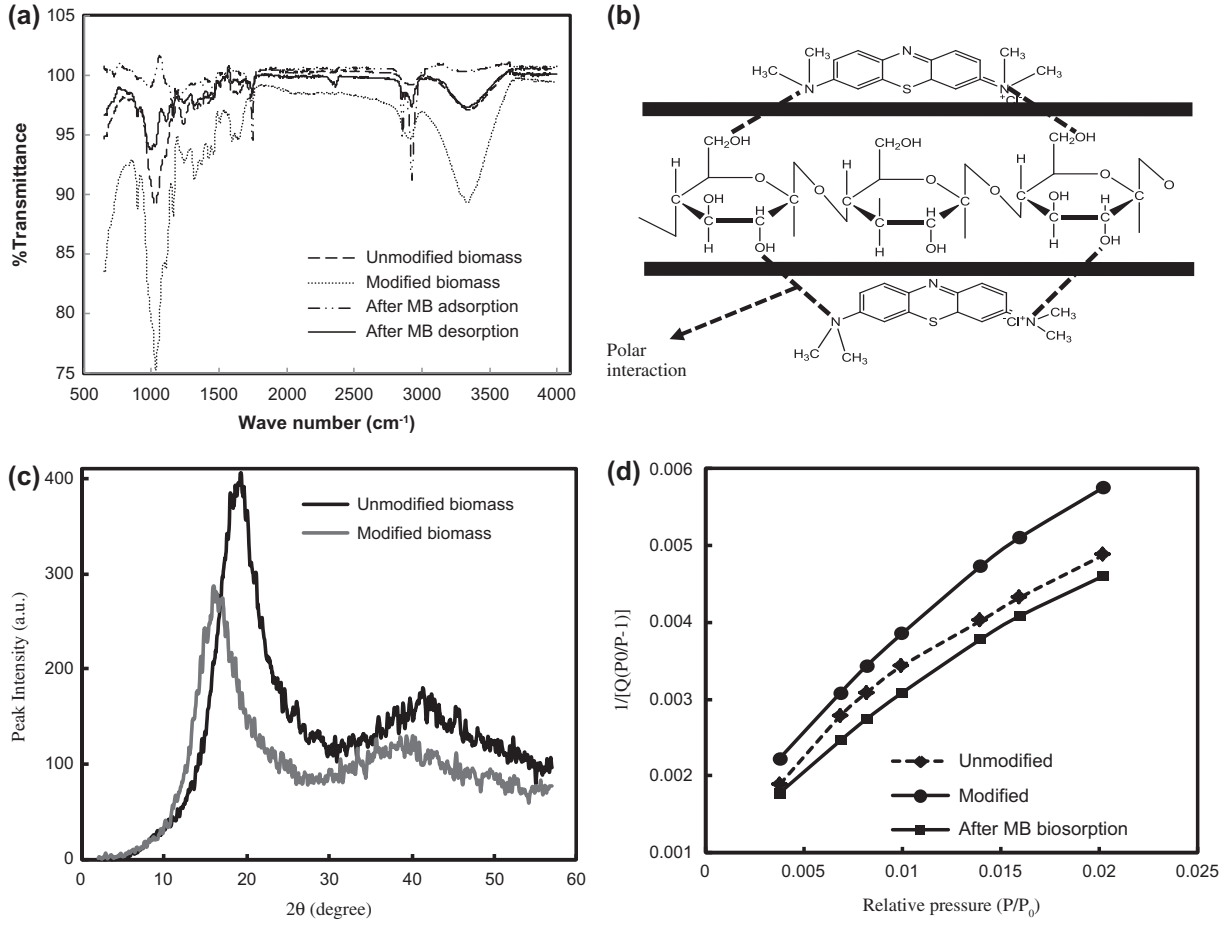

Fig. 1. FT-IR spectra of PS biomass (a), Schematic presentation for MB biosorption onto MPS (b), WXRD pattern of PS biomass (c), and BET isotherm plot of PS biomass (d).

linkages present in the modified PS [25]. In addition, the intensities of absorption bands at 3,311 and 1,026 cm^{-1} (due to the presence of $–CH_2OH$ and –OH groups) were enhanced after NaOH treatment of PS (MPS) confirming enhancement in extent of these functionalities on the surface of MPS. The existence of cellulose in MPS biosorbent was confirmed from the relatively high intensity peak at 1,026 cm^{-1} due to the stretching vibration of C–O in alcohols and phenol [26]. The obtained results proved that cellulose constituent was left in MPS biosorbent and other constituents like lignin and hemicellulose were dissolved after treatment with NaOH. The FTIR spectra of MPS biosorbent after MB biosorption and desorption were also recorded (Fig. 1(a)). The reduction in the intensity of absorption bands at 3,311 and 1,026 cm^{-1} was observed after biosorption. Subsequently, these peaks were appeared again with relatively less intensity after MB desorption from MPS. This confirmed that MB biosorption on the MPS was occurred through a hydrogen bonding between the acidic oxygen groups (O–H and phenolic) on MPS and nitrogen atoms present in MB. Schematic presentation of MB biosorption onto MPS biosorbent was depicted in Fig. 1(b). The possible mechanism for MB biosorption on the MPS biosorbent, which was also occurred by MB—hydrogen ion-exchange process as follows:

$$\text{Pistachio} - \text{OH} \leftrightarrow \text{Pistachio} - \text{O}^- + \text{H}^+$$

$$\text{Pistachio} - \text{O}^- + \text{MB}^+ \leftrightarrow \text{Pistachio} - \text{O} - \text{MB} + \text{H}^+$$

The SEM images of PS biosorbent before and after NaOH treatment is shown in Fig. 2. The surface roughness of PS biomass enhanced after treatment with NaOH because hemicelluloses and lignin were dissolved [27]. In addition, energy dispersive X-ray (EDX) study was conducted to investigate the

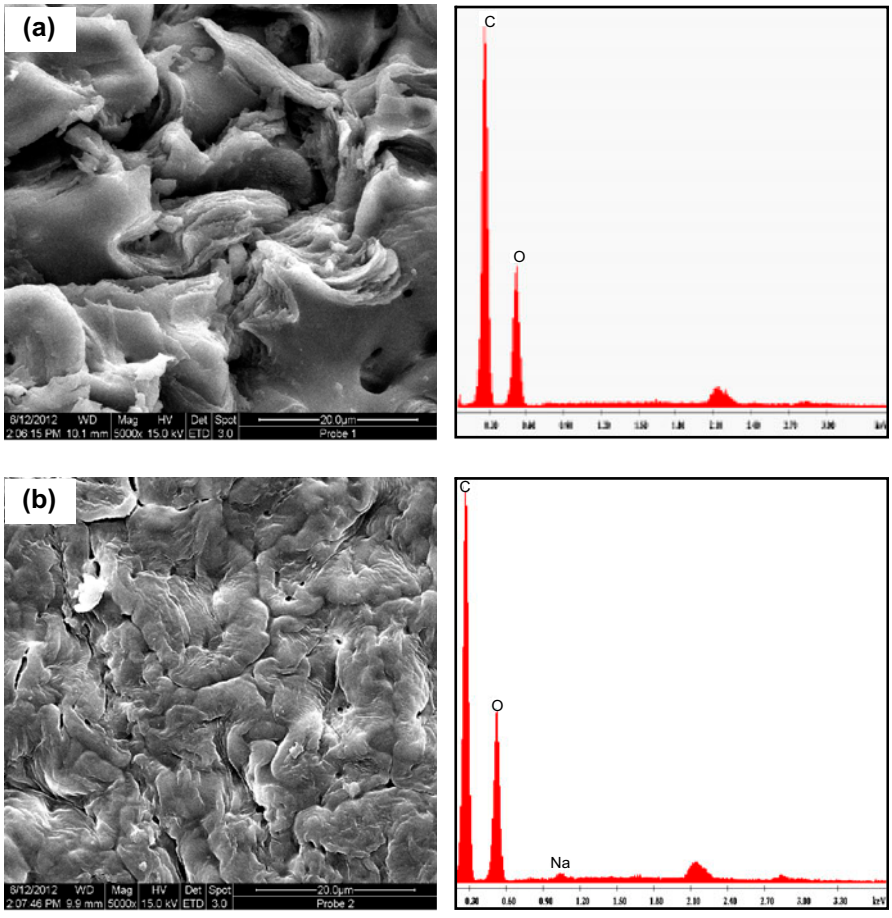

Fig. 2. SEM and EDX of PS unmodified (a), NaOH modified (b).

influence of NaOH treatment on the elemental composition of MPS. The extent of oxygen, hydrogen and carbon atoms on MPS was enhanced after treatment with NaOH. This revealed that the extent of C=O and O–H groups on the MPS was increased. The WXRD patterns of PS before and after NaOH treatment are depicted in Fig. 1(c). The intensity of peak for PS biosorbent after treatment with NaOH was reduced, which confirmed that amorphous nature of MPS biosorbent was improved because lignin and hemicellulose constituents were leached out.

The nitrogen adsorption/desorption isotherm experiments were performed to determine BET surface areas, pore volumes and pore sizes of PS biosorbent before and after NaOH treatment and MB biosorption (Table 1 and Fig. 1(d)). The BET surface area of MPS was higher than UPS because pore volume and pore size were enhanced after treatment with NaOH. In addition, BET surface area of MPS after MB biosorption decreased, confirming MB biosorption on the MPS.

3.2. Effect of ionic salt

The domestic and industrial discharges generally contain higher concentration of ionic salts, so it is essential to test the performance of biosorbent in presence of ionic salts. In this study, the biosorption performance of MPS was evaluated in presence of NaCl at various concentrations. Drastic decrease in MPS biosorption capacity from 21.6 to 2.75 mg/g was observed with increase in NaCl concentration from 0.05 to 0.25 M (Fig. 3(a)). This could be attributed to the competitive effect between MB and Na^+ to occupy the available sites on MPS surface [28]. Another probable reason for decreasing in biosorption capacity of MPS in presence of ionic salt may be slight increase in dissociation of adsorbate and an enhanced aqueous solubility. Similar effect for MB biosorption from

Table 1
Surface characteristics of biomass

Biosorbent	BET surface area (m^2/g)	Pore volume (cm^3/g)	Pore size (nm)
UPS	23.71	0.102	1.03
MPS	35.57	0.282	1.69
After MB biosorption	18.48	0.178	0.97

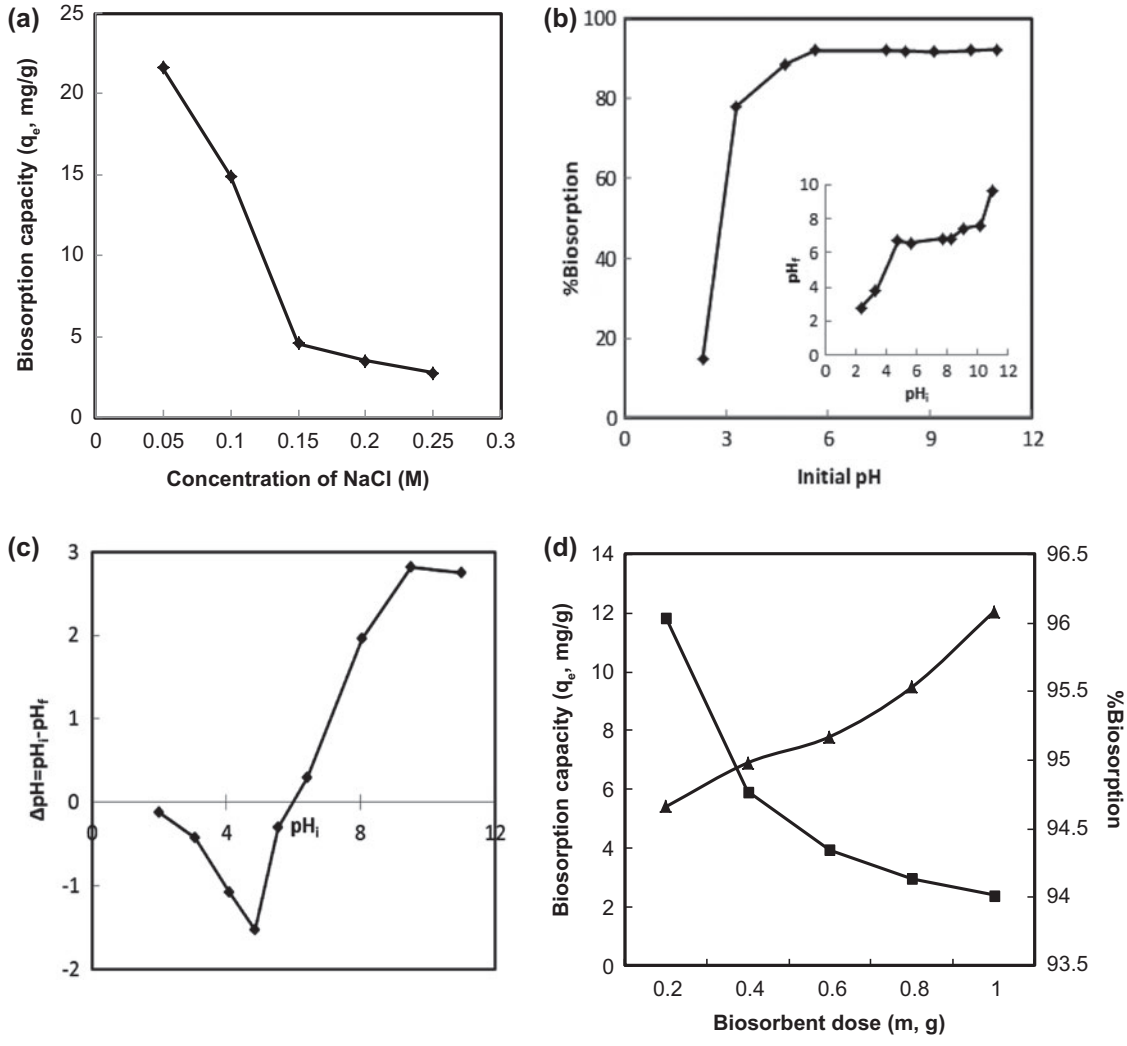

Fig. 3. Effect of ionic salt on MB biosorption on MPS (a), Effect of pH on MB biosorption on MPS (b), Point of zero charge (pH_{PZC}) plot of MPS using NaCl (0.10 M) (c), and Effect of MPS dose on MB biosorption (d). Conditions: (a) C_o–100 mg/L, temperature–298 K, agitation speed–120 rpm, contact time–24 h. (b) Co–25 mg/L, temperature–298 K, agitation speed–120 rpm, contact time–24 h. (d) Co–100 mg/L, temperature–298 K, agitation speed–120 rpm, contact time–24 h.

aqueous solution on the biosorbent was reported elsewhere [29].

3.3. Effect of pH

The solution pH is a critical parameter which governs the biosorption efficiency of biosorbent because solution pH may affect the surface charge of biosorbent, degree of ionization of adsorbate, dissociation of functional groups onto the active sites of the biosorbent and the structure of the adsorbate molecule. In this study, a profound effect of solution pH was observed on MB biosorption onto the MPS biosorbent. Biosorption of MB onto the MPS

biosorbent increased from 14.68 to 92.12% as initial solution pH increased from 2.32 to 10.98 (Fig. 3(b)). Optimum biosorption of MB [92.12%] was observed at pH: 5.63. Surface charge studies for determining point of zero charge [pH_{PZC}] of MPS were carried out by solid addition method (Fig. 3(c)) [30]. The observed pH_{PZC} of MPS was ~6.0. At lower pH values, the surface of biosorbent was highly protonated and electrostatic repulsive forces dominate between MB and MPS. However, the surface of MPS was positively charged below pH_{PZC} [pH_{PZC} 6.0] opposing MB biosorption. The biosorption of MB onto MPS biosorbent improved with increase in solution pH due to the reduction in the number of proton in aqueous medium. It was observed that the final pH [pH_f] was higher than the pH_i at equilibrium for initial pH (pH_i): 2.32–7.72 range, whereas the pH_f was lower than the pH_i 8.27–10.98 range at equilibrium (Fig. 3(b)). This indicates that MPS has buffering capacity in acid and alkaline mediums [10].

3.4. Effect of biosorbent dose

Biosorption of MB onto MPS was tested by varying the amount of MPS from 0.20 to 1.0 g at 100 mg/L initial MB concentration and pH ~6.0. Increase in MB biosorption from 94.66 to 96.08% was observed with increase in MPS dose (Fig. 3(d)). The increase in percentage of biosorption of MB is due to the increase in active sites onto the surface of biosorbent and the high surface area [30]. Moreover, the decrease in biosorption capacity of MPS was observed from 11.83 to 2.4 mg/g with increase in MPS dose. This might be due to the fact that some of the biosorption sites may remain unsaturated during the process.

3.5. Effect of contact time and biosorption kinetics

Contact time studies were conducted by varying initial MB concentrations (25–100 mg/L). The increase in biosorption capacity from 5.75 to 23.07 mg/g for aforementioned MB concentration range was observed (Fig. 4). Initially, MB biosorption at various initial MB concentrations on MPS surface was very fast as revealed from the steep slope. The probable reason for the fast biosorption of MB onto the MPS at the initial stage of process might be the availability of more binding sites onto the surface of MPS. Biosorption of MB on MPS gradually decreases and attains plateau zone at equilibrium with increase in contact time. Saturation of binding sites on MPS surface and steric repulsion between the solute molecules could ensue and slow down MB biosorption [31]. The equilibration

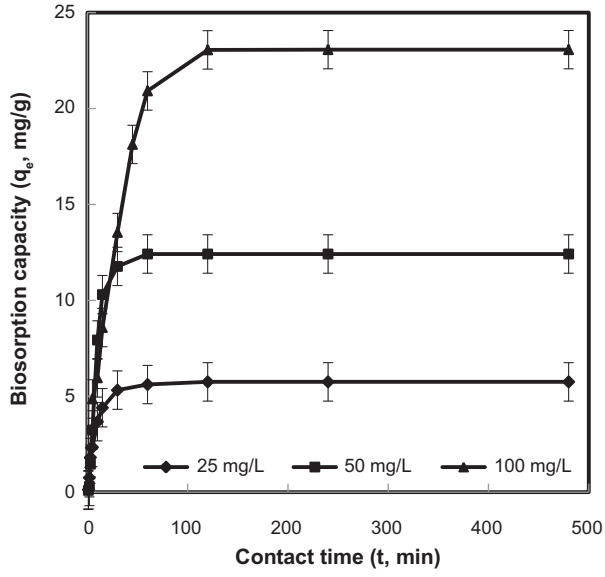

Fig. 4. Effect of contact time on MB biosorption on MPS. (Conditions: temperature—298 K, agitation speed—120 rpm, pH_i ~6).

time for MB biosorption on MPS at various initial MB concentrations varied between 60 and 240 min.

Pseudo-first-order and pseudo-second-order kinetic models were applied to kinetics data. Pseudo-first-order kinetic model [32] in linearized form is given by Eq. (3):

$$\log(q_e - q_t) = \log q_t - \frac{K_1}{2.303} \times t \tag{3}$$

where, q_e and q_t (mg/g) are the biosorption capacities at equilibrium and at any time t(min) and K_1 (1/min) is pseudo-first-order rate constant. The pseudo-second-order kinetic model [33] in linearized form is expressed by using Eq. (4):

$$\frac{t}{q_t} = \frac{1}{K_2 q_e{}^2} + \frac{1}{q_t} \times t \tag{4}$$

where, K_2 is pseudo-second-order rate constant (g/mg-min). The normalized standard deviation ($\Delta q\%$) was calculated to testify the quantitative accuracy of kinetics data. The normalized standard deviation is given by Eq. (5):

$$\Delta q(\%) = 100\sqrt{\left(\frac{\sum\left[(q_{t,\exp} - q_{t,\mathrm{cal}})/q_{t,\exp}\right]^2}{N-1}\right)} \tag{5}$$

where, the $q_{t,\exp}$ and $q_{t,\mathrm{cal}}$ are experimental and calculated biosorption capacity values at time t and N is the

number of data points. Biosorption kinetics results showed that pseudo-second-order kinetic model was better applicable to biosorption data as revealed from higher correlation coefficient (R^2) values (Table 2) and nearer $q_{e,\exp}$ and $q_{e,\text{cal}}$ at different concentrations. The validity of pseudo-second-order kinetic model was further confirmed from lower $\Delta q(\%)$ values compared to pseudo-first-order model at different concentrations.

3.6. Effect of MB concentration and biosorption isotherms

Biosorption of MB as a function of concentration onto MPS at various temperatures (298–328 K) was studied. L-type isotherm was obtained at various temperatures (Fig. 5) for MB biosorption onto MPS [34]. Biosorption of MB increases with temperature suggesting the endothermic nature of the process. Biosorption of MB onto MPS rapidly increases with initial MB concentration as observed from steep slope of curves finally attaining equilibrium. This observation reveals that the surface saturation of the biomass was dependent on the initial concentration of MB solution. The biosorption of MB onto biosorption sites was rapid at low concentration of adsorbate (MB). However, at high concentration, adsorbate needs to diffuse into the biomass surface through intraparticle diffusion and hydrolysed ions were diffused into the biomass surface at slower rate [35]. Non-linear Langmuir, Freundlich, Redlich-Peterson (R–P) and Sips isotherm models were applied to biosorption data as in certain cases linearized isotherm models would alter the regression results, influencing its accuracy and consistency. Moreover, linear models assume that the scatter vertical points around the line follow a Gaussian distribution, and the error distribution is uniform at each value of the liquid phase residual concentration (*X*-axis). The equilibrium relationship is impossible as the isotherm models have non-linearized in shapes and the error distribution tends to get altered after transformation into a linearized form [36].

Langmuir isotherm is an empirical model and assumes monolayer biosorption onto biosorbent surface. The biosorption occurs at a finite number of localized sites which are identical and equivalent with no lateral interaction and steric hindrance between the adsorbed molecules even onto adjacent sites. Langmuir isotherm in non-linearized form is given as follows (Eq. (6)) [37]:

$$q_e = \frac{q_m b C_e}{1 + bC_e} \tag{6}$$

where, q_m (mg/g) and b (L/mg) are Langmuir constants which represent maximum monolayer biosorption of MB onto MPS biosorbent and adsorption energy. The favourability of biosorption process was determined from a dimensionless constant known as separation factor (R_L) given as (Eq. (7)):

$$R_L = \frac{1}{1 + bC_o} \tag{7}$$

If, $R_L > 1$—unfavourable adsorption, $0 < R_L < 1$– favourable, $R_L = 0$—irreversible and $R_L = 1$—linear.

Freundlich model is applied to multilayer biosorption process. The distribution of biosorption heat and affinities over the heterogeneous surface is non-uniform. Non-linearized form of Freundlich isotherm is given as (Eq. (8)) [38]:

$$q_e = K_F C_e^{1/n} \tag{8}$$

where, K_F (mg/g)(L/mg)$^{1/n}$ and n are Freundlich constants measuring the biosorption capacity and biosorption intensity. The magnitude of Freundlich constant (n) determines the favourability of biosorption process. The value of $1/n$ between 0 and 1 indicates favourable adsorption and the approach of values towards zero implies an increase in heterogeneity of surface.

Redlich–Peterson (R–P) is a three parameter empirical model, a hybrid isotherm featuring both Langmuir and Freundlich isotherms. The R–P model has a linear dependence on concentration in the numerator and an

Table 2
Kinetics data for MB biosorption onto MPS

		Pseudo-first-order kinetics				Pseudo-second-order kinetics			
C_0 (mg/L)	$q_{e,\exp}$ (mg/g)	$q_{e,\text{cal}}$ (mg/g)	K_1 (1/min)	R^2	Δq (%)	$q_{e,\text{cal}}$ (mg/g)	K_2 (g/mg-min)	R^2	Δq (%)
25	5.75	4.52	0.0631	0.9572	21.39	5.93	0.0161	0.9932	3.03
50	12.42	14.08	0.1073	0.9830	13.36	13.81	0.0020	0.9149	11.19
100	23.07	46.74	0.0649	0.9480	102.60	24.33	0.0021	0.9971	5.46

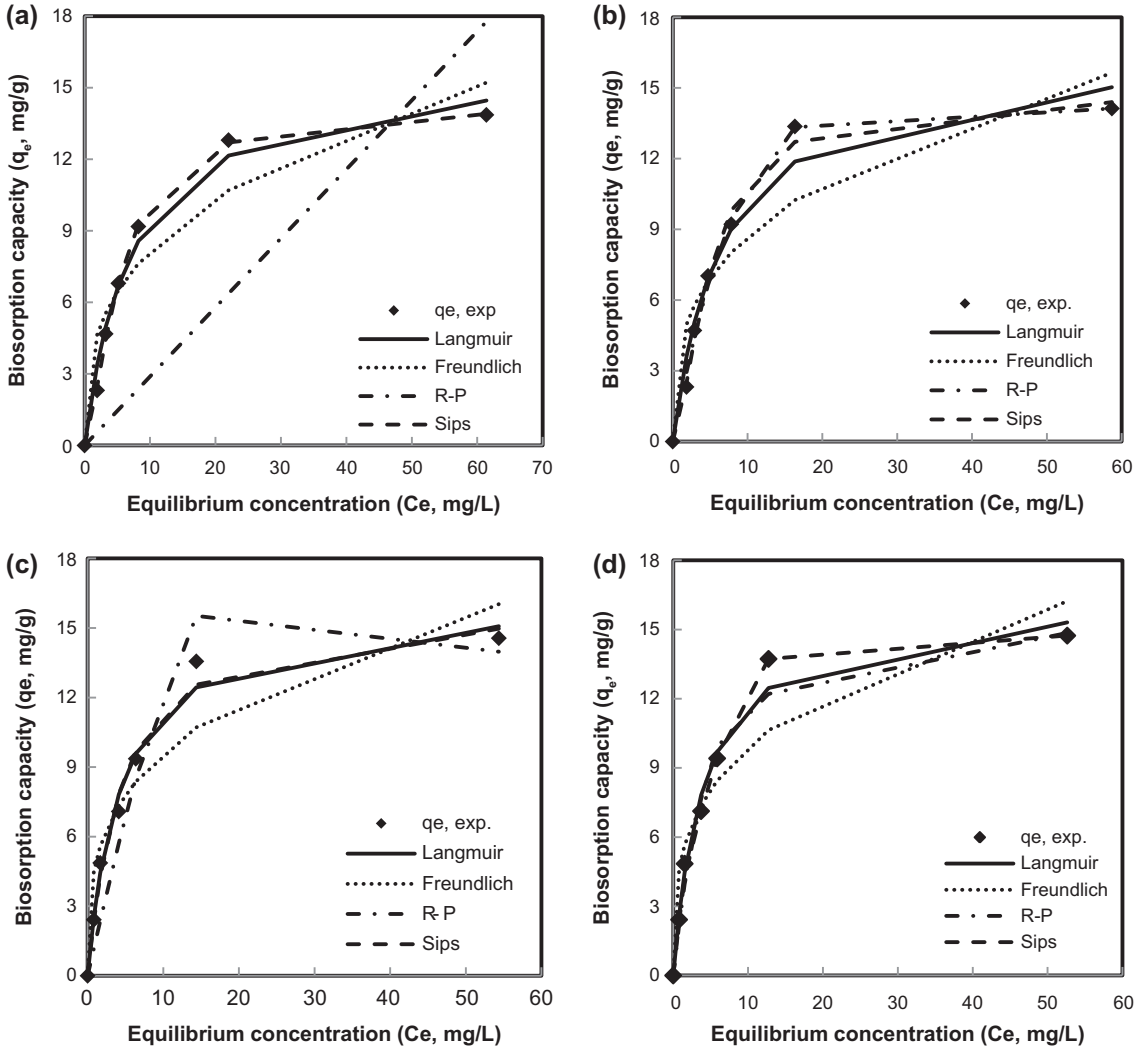

Fig. 5. Non-linear biosorption isotherm at different temperatures: 298 K (a), 308 K (b), 318 K (c), and 328 K (d).

exponential function in the denominator to represent biosorption equilibrium over a wide range of concentration. This model can be applied in homogeneous or heterogeneous systems and mathematically it is expressed as follows (Eq. (9)) [36, 39]:

$$q_e = \frac{K_R C_e}{1 + a_R C_e^{\beta}} \tag{9}$$

where, K_R (mg/g) and a_R (mg/g$^{\beta}$) are R–P constants and β is the R–P isotherm exponent, lies between 0 and 1. If $\beta = 1$, R–P isotherm will covert to Langmuir isotherm, $a_R C_e^{\beta} >> 1$, R–P isotherm will be changed to Freundlich isotherm and $a_R C_e^{\beta} << 1$, R–P isotherm will be reduced to Henry's law.

Sips isotherm, a conjugation of Langmuir and Freundlich isotherm deduced for predicting the heterogeneous adsorption systems and circumventing the limitation of the rising adsorbate concentration associated with Freundlich model. At low concentrations, it reduces to Freundlich isotherm while, at high concentrations, it predicts a monolayer adsorption capacity characteristic of Langmuir isotherm [36]. Sips isotherm in non-linear form is given as (Eq. (10)) [40]:

$$q_e = \frac{Q_s K_s C_e^{n_S}}{1 + K_s C_e^{n_S}} \tag{10}$$

where Q_s (mg/g) and K_s (L/mg)^n are Sips maximum biosorption capacity and Sips equilibrium constant and n_s is Sips model exponent. Non-linear isotherm parameters for aforementioned models were evaluated using Microsoft Excel SOLVER software. The optimization procedure requires an error function for

evaluating the fit of equation to the experimental data. The residual or sum of squares error (SSE) used as an error function to measure the fit of equation is given as (Eq. (11)):

$$\mathrm{SSE} = \sqrt{\left(\frac{\sum \left(q_{e,\exp} - q_{e,\mathrm{cal}}\right)^2}{N}\right)} \quad (11)$$

where, N is number of data points, $q_{e,\exp}$ (mg/g) is adsorbed amount of adsorbate at equilibrium obtained from experiment and $q_{e,\mathrm{cal}}$ (mg/g) is adsorbed amount of adsorbate at equilibrium obtained from the models (mg/g).

Biosorption isotherm parameters are tabulated in Table 3. Sips model fits well to the experimental data at various temperatures as obtained high value of R^2 (Fig. 5). The suitability of Sips model confirms that biosorption MB onto MPS was both homogeneous and heterogeneous. The obtained values of $1/n$ were in between 0 and 1 at various temperatures favour the suitability of the biosorption process. Moreover, the surface heterogeneity increased with temperature as confirmed from decrease in $1/n$ values. The R_L values in between 0 and 1 support the favourable biosorption process. The maximum monolayer biosorption capacity obtained was compared with other biosorbents (Table 4).

3.7. Biosorption thermodynamics

Thermodynamics studies were conducted out by varying reaction temperature in range 298–328 K and initial MB concentration (25–200 mg/L). The increase in biosorption of MB onto MPS with rise in temperature confirms that biosorption process was endothermic process (Fig. 6(a)). The increase in biosorption with rise in reaction temperature might be due to: (i) the reduction in aqueous phase viscosity (increasing mobility of MB molecules), and (ii) an increase in diffusion rate of MB molecules across the external boundary layer and the internal pores of MPS biomass. In addition, swelling in internal structure of MPS biomass might be another probable reason for increase in biosorption capacity [47]. The increase in biosorption capacity of MPS with temperature was significantly observed at high concentrations of MB (i.e. 150 and 200 mg/L). Analysis of variance (ANOVA: Single Factor) using Analysis tool Pack of Microsoft Office 2010 was carried out to justify the

Table 3
Non-linear isotherms parameters for MB biosorption onto MPS

Isotherms	Parameters	Temperature (K)			
		298	308	318	328
Langmuir	b(L/g)	0.1372	0.1497	0.2235	0.2420
	q_m(mg/g)	16.174	16.742	16.315	16.510
	SSE	2.3646	4.8694	2.3024	2.6715
	R_L	0.035–0.226	0.032–0.210	0.022–0.152	0.020–0.142
	R^2	0.9770	0.9550	0.9814	0.9789
Freundlich	K_f(mg/g)(L/mg)$^{1/n}$	3.7064	4.0621	4.7823	4.9861
	$1/n$	0.3429	0.3312	0.3026	0.2978
	SSE	14.86	21.70	16.19	18.39
	R^2	0.8556	0.8016	0.8580	0.8434
R–P	K_R(mg/g)	1.1972	1.6894	1.4226	3.0306
	a_R(mg/g$^{\beta}$)	0.8507	0.0246	0.0015	0.1048
	β	1.0000	1.3506	1.0000	1.1434
	SSE	148.1	0.6891	14.579	1.6514
	R^2	0.6268	0.9941	0.9241	0.9878
Sips	Q_s(mg/g)	14.2688	14.6967	15.9465	15.9882
	K_s(L/mg)^{n}	0.0783	0.0785	0.2122	0.2247
	n_s	1.5021	1.5765	1.0727	1.1200
	SSE	0.0967	1.0388	2.2014	2.4326
	R^2	0.9991	0.9913	0.9826	0.9814

Table 4
Comparison of MB maximum monolayer biosorption capacity with different biomass

Biosorbent	Experimental conditions	Maximum monolayer biosorption capacity (q_m, mg/g)	Refs.
Hazelnut shell activated carbon	150 rpm, 24 h	8.82	[41]
Corncob activated carbon	30°C, 5 days	0.84	[42]
Lemon peel	305 K	33.17	[43]
Wheat shells	60 min, 303 K	16.56	[44]
$CaCl_2$ treated Beech sawdust	23°C, 14 days	13.02	[45]
Cereal chaff	100 rpm, 298 K	20.3	[46]
MPS	308 K, 120 rpm, 24 h	16.74	This study

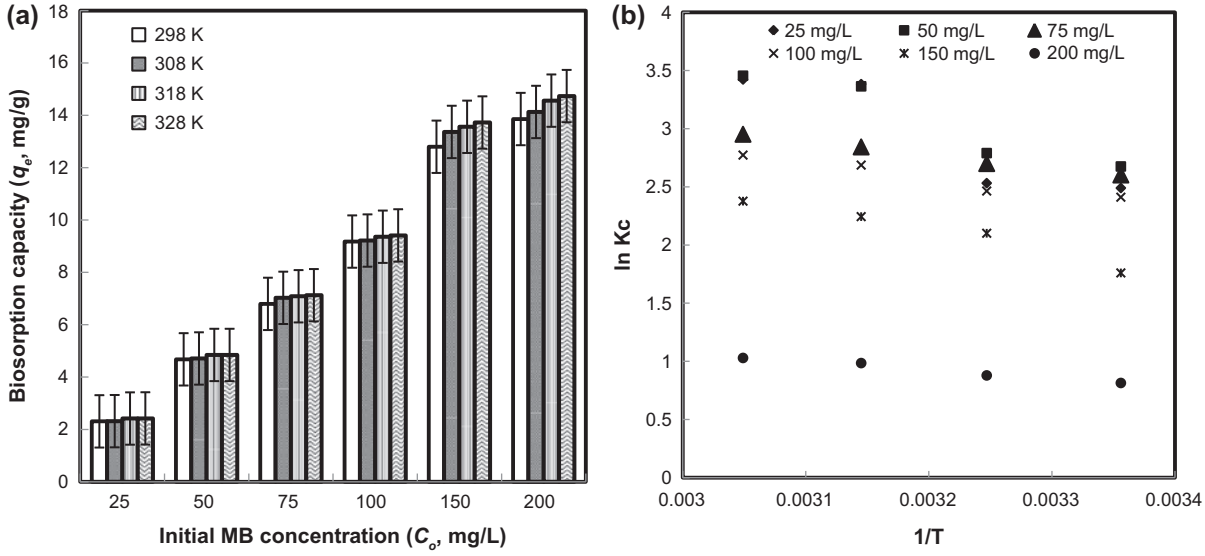

Fig. 6. Effect of temperature on MB biosorption (a), Van't Hoff plot for MB biosorption on MPS (b).

accuracy to obtained biosorption capacity values at different temperature. An alpha (α) level of 0.05 was set to determine the statistical significance in analysis. Results showed F and P-values as 0.0105 and 0.9985, respectively. These values were well less than F_{crit} value (3.0984) confirming significance of data.

Thermodynamics parameters such as standard enthalpy change (ΔH°), standard entropy change (ΔS°) and standard free energy change (ΔG°) were determined. The ΔH° and ΔS° values were calculated with the help of Van't Hoff plot (Fig. 6(b)). The equation is expressed as follows (Eq. (12)):

$$\ln k_c = \frac{\Delta S^\circ}{R} - \frac{\Delta H^\circ}{RT} \tag{12}$$

where R (8.314 J/mol-K) is the universal gas constant, T(K) is the absolute temperature and k_c is a constant, given as (Eq. (13)):

$$k_c = \frac{C_{Ae}}{C_e} \tag{13}$$

where, C_{Ae} and C_e are MB equilibrium concentration on the biosorbent and in the solution, respectively.

Gibb's free energy change (ΔG°) was calculated using the following relation (Eq. (14)):

$$\Delta G^\circ = -RT \ln k_C \tag{14}$$

The calculated thermodynamic parameters are given in Table 5. The negative ΔG° values indicate that the biosorption of MB onto MPS was spontaneous. Moreover, the decrease in ΔG° values observed with increase in temperature which favors the biosorption of MB biosorption onto MPS at high temperature. The positive ΔH° values confirm that the biosorption process is endothermic. The positive ΔS° values reflect the

Table 5
Thermodynamics parameters for MB biosorption onto MPS

	ΔS° (J/mol-K)	ΔH° (kJ/mol)	$-\Delta G^\circ$ (kJ/mol)			
			298 K	308 K	318 K	328 K
25	119.38	29.63	6.17	6.49	8.95	9.34
50	101.26	23.67	6.63	7.15	8.90	9.42
75	54.05	9.68	6.45	6.92	7.52	8.05
100	55.43	10.61	5.97	6.31	7.11	7.56
150	69.79	16.30	4.36	5.38	5.93	6.48
200	27.25	6.11	2.02	2.25	2.61	2.81

affinity of MPS towards MB. Similar observation for MB biosorption was reported elsewhere [39]. To evaluate the nature of biosorption process, Dubinin–Radushkevich (D–R) isotherm was applied to biosorption thermodynamics data. D–R isotherm in linearized form is given as (Eq. (15)) [47]:

$$\ln q_e = \ln q_m - \beta\varepsilon^2 \tag{15}$$

where, β and ε are activity coefficient constants, which are related to biosorption energy (mol^2/J^2) and Polyanyi potential.

The activity coefficient constant is given as (Eq. (16)):

$$\varepsilon = RTln\left(1 + \frac{1}{C_e}\right) \tag{16}$$

The q_m and β values were calculated from the intercept and slope of a plot between ln q_e and ε^2 (figure not shown). The mean free energy (E_a, kJ/mol) can be calculated as (Eq. (17)):

$$E_a = \frac{1}{\sqrt{(-2\beta)}} \tag{17}$$

The magnitudes of E_a at various temperatures were in range 7.071–7.905 kJ/mol, reflecting physical nature of biosorption. The physical nature of biosorption process was further confirmed from the obtained ΔH° values at different MB concentrations (i.e. <40 kJ/mol) [48].

3.8. Desorption and regeneration studies

It is essential to perform desorption and regeneration studies to elucidate the economic feasibility of biosorption process by retaining adsorbate for its reusability and biosorbent repeatedly. In this study, MB optimum elution (93.5%) was observed in 0.10 M OA (Fig. 7(a)) while, 14.6, 6.4, and 49.7% MB was recovered in MeOH, EeOH and Ac, respectively. To

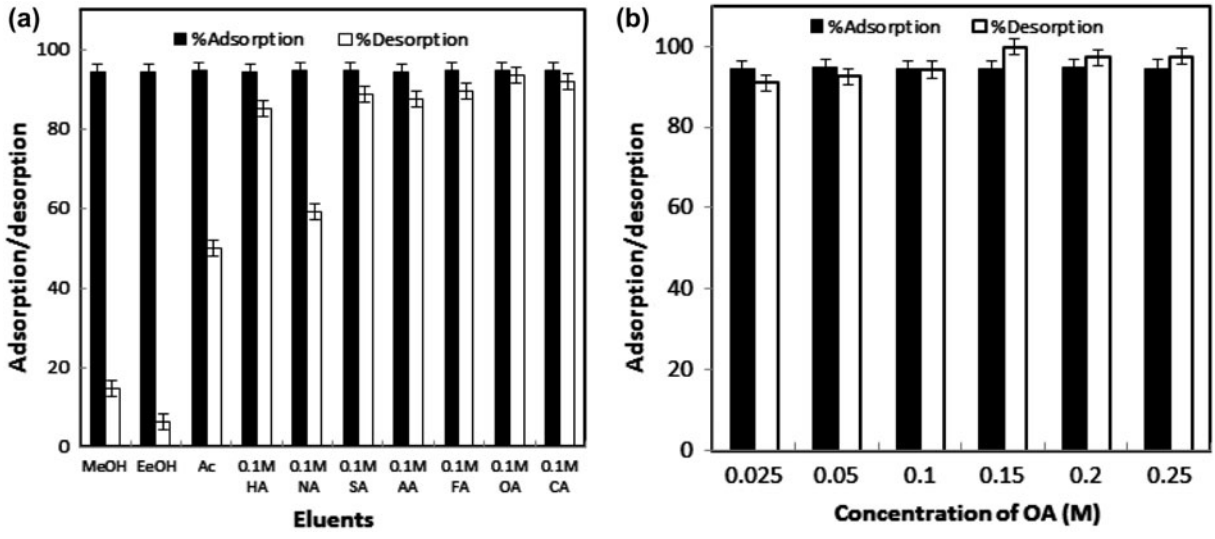

Fig. 7. Desorption of MB using different eluents (a), and at various concentrations of oxalic acid (b).

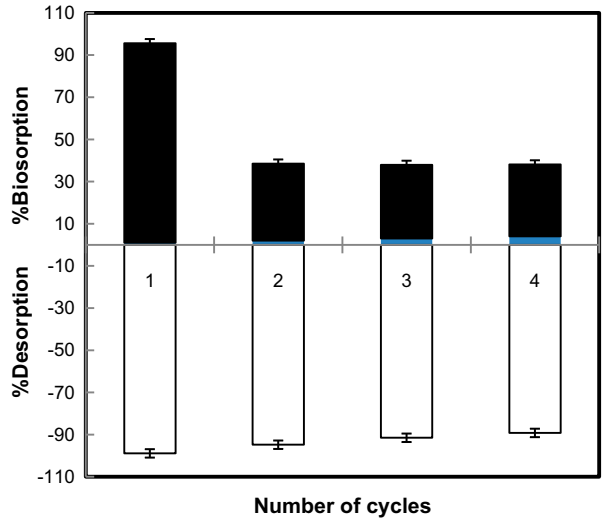

Fig. 8. Regeneration studies plot.

evaluate the effect of OA concentration on MB recovery from MPS experiments were conducted by varying the concentration of OA in the range 0.025–0.25 M (Fig. 7(b)). The 99.8% MB was recovered in 0.15 M OA in 15 min. Regeneration studies showed almost constant recovery rate for four consecutive cycles which confirms the economic feasibility of MPS as biosorbent for the removal of MB from aqueous solution and wastewater. The drastic drop in biosorption rate from 94.6 to 36.5% was observed after first cycle (Fig. 8). This might be due to the loss in active sites of MPS after acid treatment, which are responsible for MB biosorption. In addition, biosorption rate was further stagnant for consecutive cycles.

4. Conclusions

Batch mode MB biosorption onto MPS was investigated. Studies revealed decrease in PS crystallinity after NaOH treatment and biosorption of MB enhanced from 57 to 92%. The NaOH treated PS (MPS) biosorbent had greater BET surface area (35.57 m^2/g) and more active sites for MB biosorption from aqueous solution. The biosorption of MB onto MPS occurred through a hydrogen bonding between acidic oxygen surface groups and MB nitrogen atoms. The profound effect of ionic salt, solution pH and biosorbent dose was observed on MB biosorption onto MPS. Contact time studies at various initial MB concentrations showed variation in equilibration time from 60 to 240 min. The MB biosorption from aqueous solution followed the pseudo second order kinetic model. Biosorption isotherm experiments revealed that MB biosorption from aqueous solution was well fitted for Sips model. Freundlich constant (n) and separation factor (R_L) values indicated favourable biosorption process. Thermodynamics study showed endothermic and physical process. The MB recovery was 99.8% with 0.15 M OA in 15 min. Regeneration studies showed almost constant recovery rate for four consecutive cycles which confirms the economic feasibility of MPS as biosorbent for MB removal from aqueous solution and wastewater.

Acknowledgements

Authors would like to acknowledge Deanship of Scientific Research (RGP-VPP-052) at King Saud University, Riyadh.

References

[1] A. Srinivasan T. Viraraghavan, Decolorization of dye wastewaters by biosorbents: A review, J. Environ. Manage. 91 (2010) 1915–1929.
[2] K.A.G. Gusmão, L.V.A. Gurgel, T.M.S. Selo, L.F. Gil, Application of succinylated sugarcane bagasse as adsorbent to remove methylene blue and gentian violet from aqueous solutions—Kinetic and equilibrium studies, Dyes Pigm. 92 (2012) 967–974.
[3] M. Wainwright, K.B. Crossley, Methylene blue – A therapeutic dye for all seasons? J. Chemo. 14 (2002) 431–443.
[4] M.J. Ahmed, S.K. Dhedan, Equilibrium isotherms and kinetics modeling of methylene blue adsorption on agricultural wastes-based activated carbons, Fluid Phase Equilib. 317 (15) (2012) 9–14.
[5] M.S. Baburaj, C.T. Aravindakumar, S. Sreedhanya, A.P. Thomas, U.K. Aravind, Treatment of model textile effluents with PAA/CHI and PAA/PEI composite membranes, Desalination 288 (2012) 72–79.
[6] J. Ma, Y. Jia, Y. Jing, Y. Yao, J. Sun, Kinetics and thermodynamics of methylene blue adsorption by cobalt-hectorite composite, Dyes Pigm. 93 (2012) 1441–1446.
[7] M.A. Rauf, S.B. Bukallah, F.A. Hamour, A.S. Nasir, Adsorption of dyes from aqueous solutions onto sand and their kinetic behavior, Chem. Eng. J. 137 (2008) 238–243.
[8] D. Wu, P. Zheng, P.R. Chang, X. Ma, Preparation and characterization of magnetic rectorite/iron oxide nanocomposites and its application for the removal of the dyes, Chem. Eng. J. 174 (2011) 489–494.
[9] M. Zhao, P. Liu, Adsorption behavior of methylene blue on halloysite nanotubes, Microporous Mesoporous Mater. 112 (2008) 419–424.
[10] R.M. Reema, P. Saravanan, M. Dharmendira Kumar, Accumulation of methylene blue dye by growing lemna minor, Sep. Sci. Technol. 46(6) (2011) 1052–1058.
[11] X.-G. Chen, S.-S. Lv, S.-T. Liu, P.-P. Zhang, A.-B. Zhang, J. Sun, Y. Ye, Adsorption of methylene blue by rice hull ash, Sep. Sci. Technol. 47(1) (2012) 147–156.
[12] C. Saka, O Şahin, H. Adsoy, Ş.M. Akyel, Removal of methylene blue from aqueous solutions by using cold plasma, microwave radiation and formaldehyde treated acorn shell, Sep. Sci. Technol. 47(10) (2012) 1542–1551.

[13] L.W. Low, T.T. Teng, M.N. Rafatullah, B. Azahari, Adsorption studies of methylene blue and malachite green from aqueous solutions by pretreated lignocellulosic materials, Sep. Sci. Technol. 48(11) (2013) 1688–1698.
[14] S. Li, D. Umereweneza, Adsorption of N-vinylpyrrolidone from polyvinylpyrrolidone solution onto bamboo-based activated carbon, Sep. Sci. Technol. 47(1) (2012) 104–111.
[15] K.Y. Foo, B.H. Hameed, Preparation and characterization of activated carbon from pistachio nut shells via microwave-induced chemical activation, Biomass Bioenergy 35(7) (2011) 3257–3261.
[16] T. Kaghazchi, N.A. Kolur, M. Soleimani, Licorice residue and pistachio-nut shell mixture: A promising precursor for activated carbon, J. Ind. Eng. Chem. 16 (3) (2010) 368–374.
[17] K. Yetilmezsoy, S. Demirel, R.J. Vanderbei, Response surface modeling of Pb(II) removal from aqueous solution by *Pistacia vera* L.: Box–Behnken experimental design, J. Hazard. Mater. 171(1–3) (2009) 551–562.
[18] O. Sahin, S. Demirel, M.F. Dilekoglu, Removal of Pb(II) from Aqueous solution by antep pistachio shells, Fres. Environ. Bull. 14 (2005) 986–992.
[19] N.G. Turan, B. Mesci, Use of pistachio shells as an adsorbent for the removal of zinc(II) ion, Clean-Soil, Air, Wat. 39 (2011) 475–481.
[20] E. Bazrafshan, F.K. Mostafapour, A.H. Mahvi, Phenol removal from aqueous solutions using pistachio nut shell ash as a low cost adsorbent, Fres. Environ. Bull. 21 (2012) 2962–2968.
[21] F. Toprak, B. Armagan, A. Cakici, Systematic approach for the optimal process conditions of Reactive Red 198 adsorption by pistachio nut shell using Taguchi method, Desalin. Wat. Treat. 48 (2012) 96–105.
[22] P. Vijayalakshmi, V.S.S. Bala, K.V. Thiruvengadaravi, P. Panneerselvam, M. Palanicham, S. Sivanesan, Removal of acid violet 17 from aqueous solutions by adsorption onto activated carbon prepared from pistachio nut shell, Sep. Sci. Technol. 46 (2011) 155–163.
[23] H.-C. Hsi, R.S. Horng, T.-A. Pan, S.-K. Lee, Preparation of activated carbons from raw and biotreated agricultural residues for removal of volatile organic compounds, J. Air Waste Manage 61(5) (2011) 543–551.
[24] K.Y. Foo, B.H. Hameed, Preparation of activated carbon by microwave heating of langsat (*Lansium domesticum*) empty fruit bunch waste, Bioresour. Technol. 116 (2012) 522–525.
[25] G. Socrates, Infrared Characteristic Group Frequencies. Wiley, New York, NY, 1980.
[26] B. Peters, Prediction of pyrolysis of pistachio shells based on its components hemicellulose, cellulose and lignin, Fuel Process. Technol. 92 (2011) 1993–1998.
[27] R.C. San, J. Tomkinsona, X.F. Sun, N.J. Wang, Fractional isolation and physico-chemical characterization of alkali-soluble lignins from fast-growing poplar wood, Polymer 41 (2000) 8409–8417.
[28] R. Han, W. Zou, W. Yu, S. Cheng, Y. Wang, J. Shi, Biosorption of methylene blue from aqueous solution by fallen phoenix tree's leaves, J. Hazard. Mater. 141 (2007) 156–162.
[29] B.S. Inbaraj, B.H. Chen, Dye adsorption characteristics of magnetite nanoparticles coated with a biopolymer poly(γ-glutamic acid), Bioresour. Technol. 102 (2011) 8868–8876.
[30] R.A.K. Rao, M.A. Khan, Biosorption of bivalent metal ions from aqueous solution by an agricultural waste: Kinetics, thermodynamics and environmental effects, Colloids Surf., A 332 (2009) 121–128.
[31] R. Dhodapkar, N.N. Rao, S.P. Pande, S.N. Kaul, Removal of basic dyes from aqueous medium using a novel polymer: Jalshakti, Bioresour. Technol. 97 (2006) 877–885.
[32] S. Lagergren, K. Sven, About the theory of so-called adsorption of soluble Substances, K. Sven, Vetensk-apsakad. Handl. 24(4) (1898) 1–39.
[33] Y.S. Ho, G. McKay, The kinetics of sorption of divalent metal ions onto sphagnum moss peat, Water Res. 34 (2000) 735–742.
[34] C.H. Giles, T.H. Mac, S.N. Ewan, A. Smith Nakhawa, Studies in adsorption Part XI A system of classification of solution adsorption mechanism and in measurement of specific surface areas of solids, J. Chem. Soc. 111 (1960) 2993–3973.
[35] M.N. Jnr, A.I. Spiff, Effect of metal ion concentration on the biosorption of Pb^{2+} and Cd^{2+} by caladium bicolor (Wild Cocoyam), African J. Biotechnol. 4 (2004) 191–196.
[36] K.Y. Foo, B.H. Hameed, Insights into the modeling of adsorption isotherm systems, Chem. Eng. J. 156 (2010) 2–10.
[37] I. Langmuir, The adsorption of gases on plane surface of glass, mica and platinum, J. Ameri. Chem. Soc. 40 (1916) 1361–1403.
[38] H.M.F. Freundlich, Over the adsorption in solution, J. Phys. Chem. 57 (1906) 385–470.
[39] B.H. Hameed, A.A. Ahmad, Batch adsorption of methylene blue from aqueous solution by garlic peel, an agricultural waste biomass, J. Hazard. Mater. 164 (2009) 870–875.
[40] R. Sips, On the structure of a catalyst surface, J. Chem. Phys. 16 (1948) 490–495.
[41] A. Aygun, S. Yenisoy-Karakaş, I. Duman, Production of granular activated carbon from fruit stones and nutshells and evaluation of their physical, chemical and adsorption properties, Micropor. Mesopor. Mater. 66 (2003) 189–195.
[42] R.L. Tseng, S.K. Tseng, F.C. Wu, Preparation of high surface area carbons from Corncob with KOH etching plus CO2 gasification for the adsorption of dyes and phenols from water, Colloids Surf., A 279 (2006) 69–78.
[43] K.V. Kumar, K. Porkodi, Relation between some two- and three-parameter isotherm models for the sorption of methylene blue onto lemon peel, J. Hazard. Mater. 138 (2006) 633–635.
[44] Y. Bulut, H. Aydin, A kinetics and thermodynamics study of methylene blue adsorption on wheat shells, Desalination 194 (2006) 259–267.
[45] F.A. Batzias, D.K. Sidiras, Dye adsorption by calcium chloride treated beech sawdust in batch and fixed-bed systems, J. Hazard. Mater. B 114 (2004) 167–174.
[46] R. Han, Y. Wang, P. Han, J. Shi, J. Yang, Y. Lu, Removal of Methylene Blue from Aqueous Solution by Chaff in Batch Mode, J. Hazard. Mater. B 137 (2006) 550–557.

[47] M.M. Dubinin, L.V. Radushkevich, Equation of the characteristic curve of activated charcoal, Proceedings of Academy of Science Physical Chemistry Sect. U.S.S.R 55 (1947) 331–337.

[48] S. Wang, Z.H. Zhu, Effects of acidic treatment of activated carbons on dye adsorption, Dyes Pigm. 75 (2007) 306–314.